Supplementary Tables and Figures

Supplementary Table 1. Analysis of miRNA and miRNA* species in total RNA, AGO1 complex, and AGO2 complex in S2-NP cells. The first worksheet includes the full analysis of all miRNA genes. The second worksheet includes the subset of 38 genes exhibiting >100 miRNA reads and >10 miRNA* reads in total RNA, which were used in Figure 5A. These tables tabulate the number of miRNA and miRNA* reads in total S2NP RNA (GSM371638), S2NP AGO1-IP (GSM280088) and S2NP AGO2-IP (GSM280087) sequence datasets. Enrichments in the IP libraries were calculated with respect to their miRNA/miRNA* ratio present in total RNA.

Supplementary Table 2. Analysis of miRNA reads and miRNA* reads from S2-NP total RNA, AGO1-IP and AGO2-IP, from ovary total RNA and AGO2-IP, and from S2-Z total RNA and beta-eliminated RNA. These data were used in Figure 4C.

Supplementary Table 3. Analysis of the pairing status of miRNA and miRNA* species used in Figure 5.

Supplementary Table 4. Target searches of AGO2-loaded miRNA* species. We searched for candidate targeting of bantam*, miR-276a*, miR-184* and miR-308* on annotated mRNAs (including 5'UTRs, CDS and 3' UTRs), permitting up to two mismatches and a variable number of G:U pairs. The top worksheet summarizes the number of hits to the sense (S) and the antisense (AS) strand of mRNAs across different thresholds of G:U pairing; the data are separated by miRNA* and strand in the next eight worksheets. We did not observe substantial differences between the number of S and AS hits for each miRNA*. The large number of miR-308* hits seems to be attributable to

its high uridine content, which results in a large number of sites with a high degree of G:U pairing.

Supplementary Table 5. Sequences of DNA oligonucleotides used to clone luciferase sensors, 2'Ome oligonucleotides used for miRNA inhibition, and RNA oligos used for in vitro sorting assay.

Supplementary Figure 1. miR-184 and miR-184* target assays. Renilla luciferase sensors bearing two tandem perfect or four bulged targets for the indicated miRNA (cloned in psiCHECK2, which contains an internal control firefly luciferase gene); bulged+mut targets also contained 3 mutations in seed pairs (shown is the miR-184* mutant pattern). These were co-transfected with 2'OMe antisense oligos (ASO) and derepression of sensor activity was measured. For each construct, two sets of quadruplicate transfections were done on 2 different days and the data were pooled. Values were normalized to sensor activity in the presence of non-cognate ASO against miR-288, and mean values ± S.D. are shown. Both miR-184 and miR-184* perfect sensors were derepressed by cognate ASO; however, only miR-184 bulged sensor could be derepressed.

Supplementary Figure 2. Independent sorting of the strands of *mir-184* duplex. We used the in vitro assay described in Figure 4. miR-184 was exclusively selected by AGO1, whereas miR-184* was preferentially selected by AGO2.

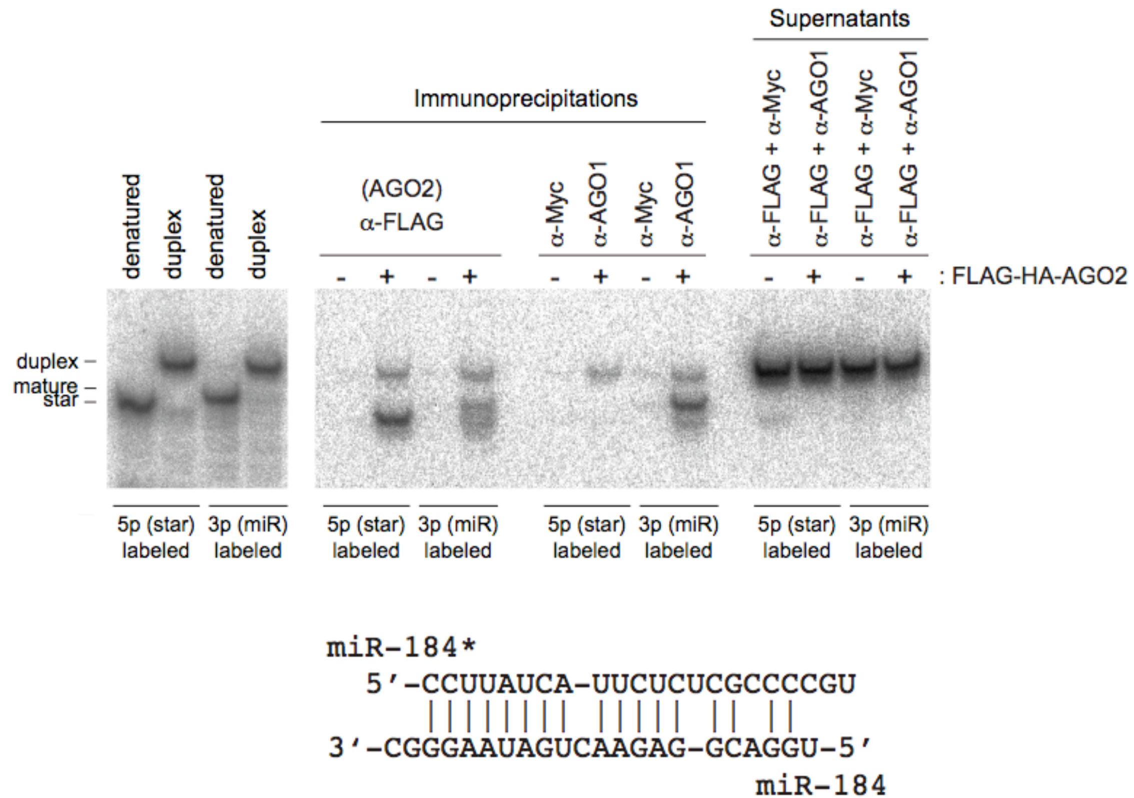

Supplementary Figure 3. Maturation of miR-276a*-programmed AGO2 complex does not require passenger strand cleavage. We introduced non-cleavable phosphorothioate (PS) linkages at the predicted site of passenger strand cleavage, and compared their in vitro sorting to wildtype *mir-276a* duplex. Maturation of single-stranded AGO2 complex was not affected by the PS substitutions.

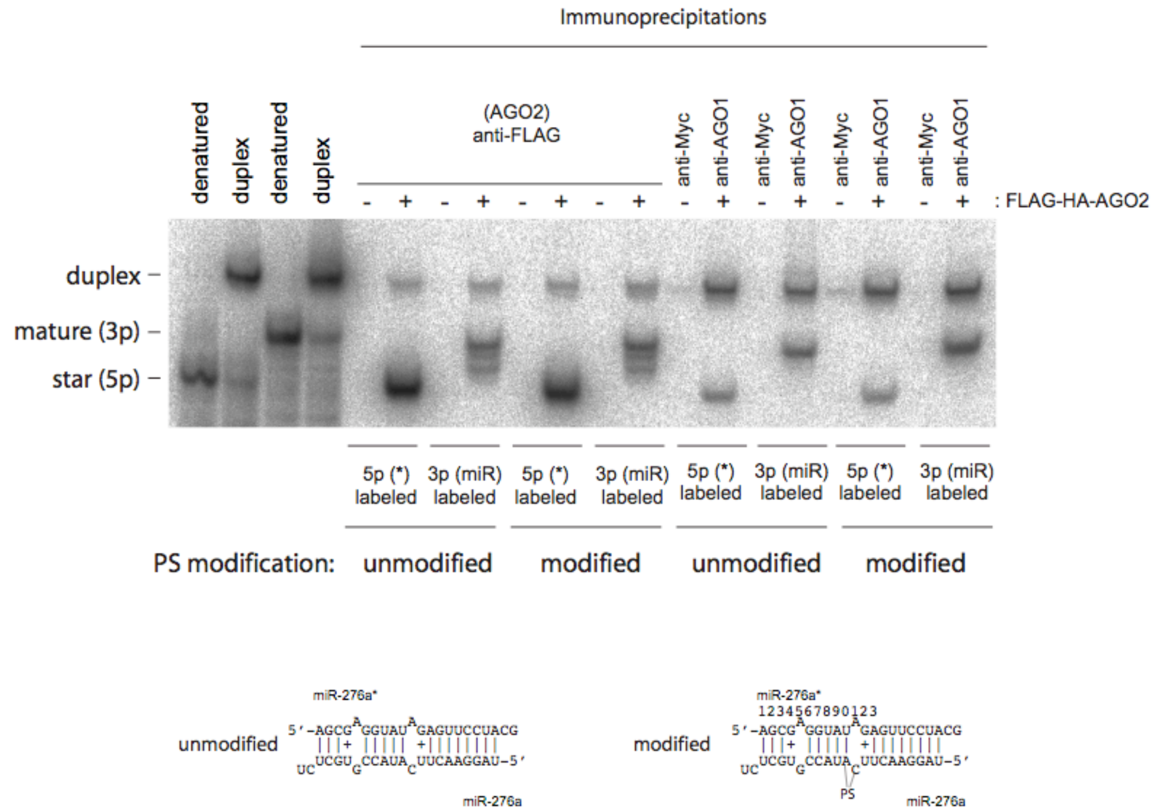

F) Supplemental Figure S1

A

Renilla luciferase

2x or 4x tandem target

perfect sensor

5'-aaaaaaNNNNNNNNNNNNNNNNNNNNNNaaaa-3'

3'-NNNNNNNNNNNNNNNNNNNNNN-5' miRNA or star

12 11 10 9 8 7 6 5 4 3 2 1

bulged sensor

5'-aaaaaaNNNNNNNNNNN NNN NNNNNNNNNNaaaa-3'

3'-NNNNNNNNNNN NNN NNNNNNNNN-5' miRNA or star

12 11 10 9 8 7 6 5 4 3 2 1

bulged+mut sensor

5'-aaaaaaNNNNNNNNNNN NNN NN N NN N N N Naaaa-3'

3'-NNNNNNNNNNN NNN NN N NN N N N N-5' miRNA or star

12 11 10 9 8 7 6 5 4 3 2 1

B

9.3x

18.6x

2'Ome-miR-288

2'Ome-miR-184

2'Ome-miR-184*

0 1 2 3 4 5

empty sensor | miR-184 perfect | miR-184 bulged | miR-184 bulged+mut | miR-184* perfect | miR-184* bulged | miR-184* bulged+mut

Supplementary Figure 1
Okamura et al

F) Supplemental Figure S2

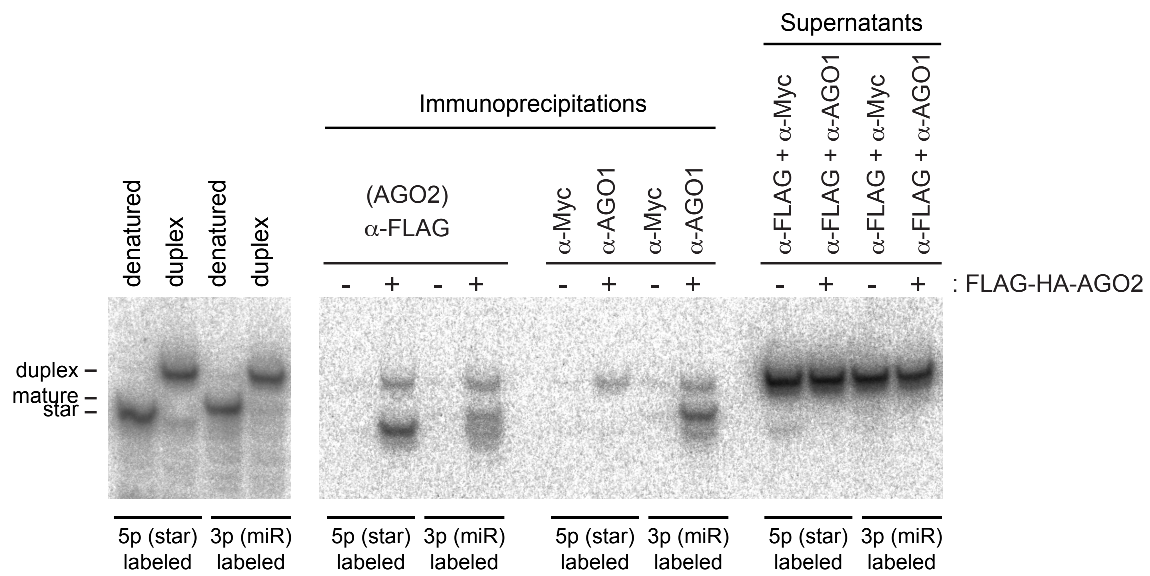

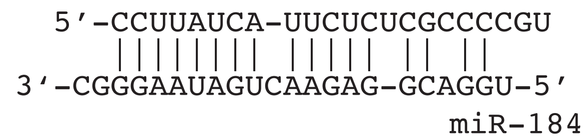

Supplementary Figure 2
Okamura et al

F) Supplemental Figure S3

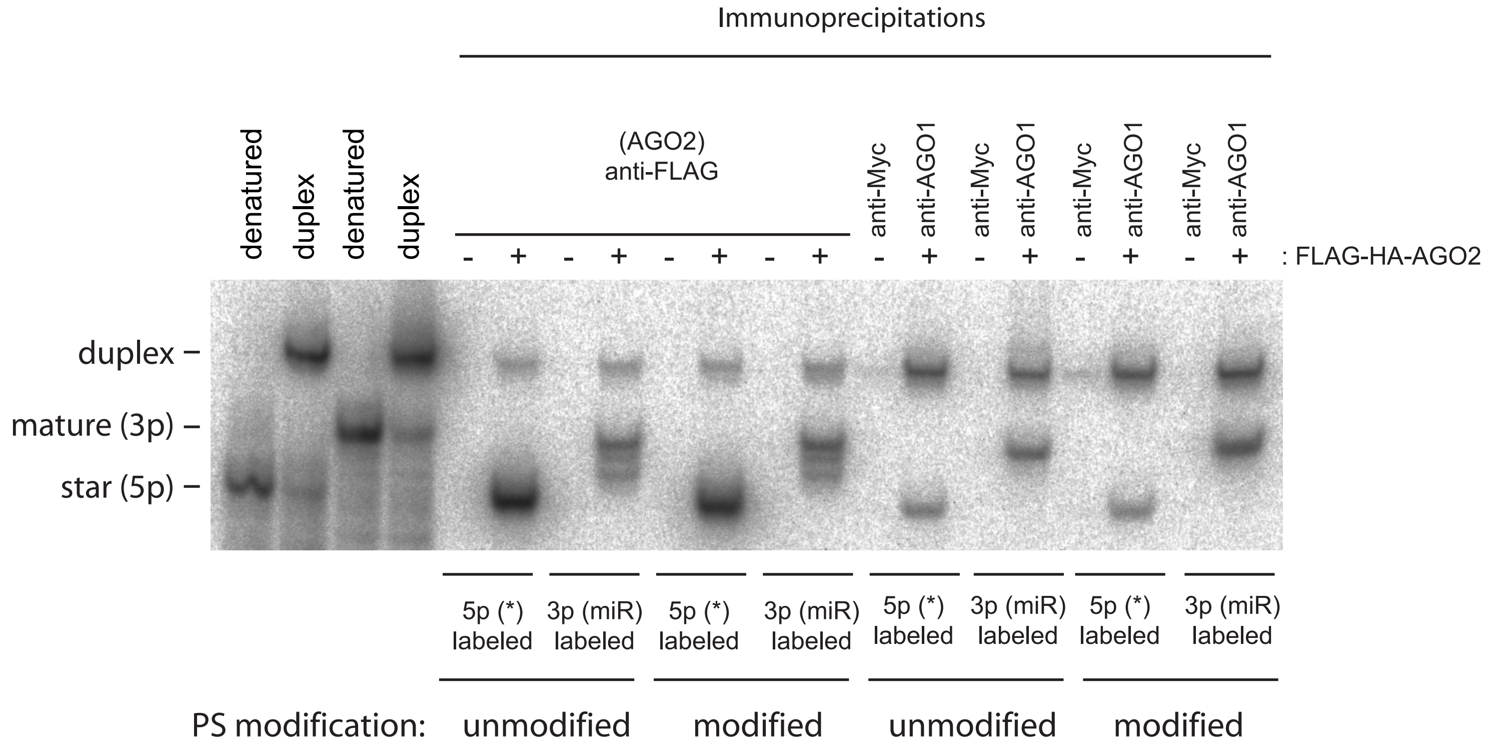

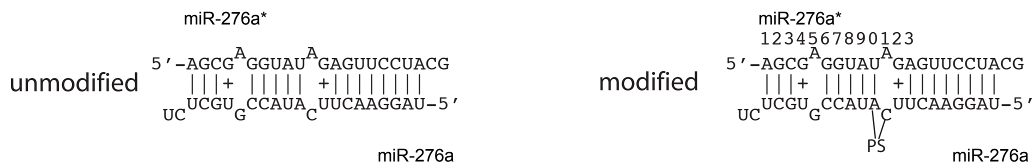

Supplementary Figure 3
Okamura et al